Cerebration Science Publishing

Cross Ventilation Enhancement in Small Dwelling Units with Double-loaded Corridor: A CFD and Field Study in Bangkok

Natthaumporn Inprom [1] and Chalermwat Tantasavasdi [1,2,*]

[1] Faculty of Architecture and Planning, Thammasat University, Pathum Thani 12121, Thailand;
ntup_ip@hotmail.com

[2] Thammasat University Research Unit in Architecture for Sustainable Living and Environment, Thammasat
University, Pathum Thani 12121, Thailand; tchalerm@engr.tu.ac.th

* Correspondence author: tchalerm@engr.tu.ac.th

Abstract: Small dwelling units in urban multi-storey buildings often suffer from inadequate ventilation due to single-sided openings, which negatively impacts thermal comfort and indoor air quality. This study investigated solutions to enhance cross ventilation, adopting a typical studio-unit layout of a Bangkok apartment as a case study. CFD simulations were conducted for 48 scenarios, varying by the internal opening design, wind direction, and unit location. Each scenario was evaluated using the average indoor velocity coefficient at occupied level (Cv_i) and the product of the velocity coefficient at openings and inlet area ($Cv_o \times A$). It was found that the base case unit (BC) provided the poorest performance (mean Cv_i = 0.01; $Cv_o \times A$ = 0.02). The improved unit with a transom window (C1) exhibited higher mean Cv_i and $Cv_o \times A$ values (0.09 and 0.26, respectively), while the unit improved with a louvre door (C2) achieved the highest values (0.20 and 0.76, respectively). The most significant parameter for improving mean Cv_i and $Cv_o \times A$ was found to be the opening design, followed by wind direction in relation to building orientation, and unit location, respectively. Further analysis based on Bangkok's climate indicated that the ventilation rate of most BC unit scenarios failed to meet the recommended criterion (5.0 ACH). In comparison, the C1 unit and C2 unit achieved ACH ranging from 12.6 to 173.7, consistently meeting the recommended criterion throughout the year across all building orientations and unit locations. Moreover, several scenarios of the C2 unit can provide occupied-level air velocities that pass the recommended criterion for thermal comfort throughout the year. The findings revealed both the potential and limitations of using internal openings for cross ventilation in compact units to improve indoor air quality and thermal comfort, providing practical solutions for architects and policymakers to enhance sustainable residential design.

Keywords: Natural ventilation; Multi-family Residential Buildings; Indoor air quality (IAQ); Thermal comfort; Wind direction; Unit location

1. Introduction

Urbanisation trends have been increasing steadily over the past 70 years, primarily in tropical developing countries, which have a significant proportion of the world's population (UN DESA 2019). Consequently, demand for dense residential buildings has risen in those urban areas (Peters & Halleran 2021; Sha & Qi 2020). Due to limited land and economic constraints, multi-family residential buildings with double-loaded corridor are being increasingly built to optimise space (Kumar et al. 2021; Fu et al. 2024). This configuration typically allows for a limited opening area only on the exterior wall of each small dwelling unit, resulting in single-sided ventilation (Prajongsan & Sharples 2012). This ventilation type leads to inadequate airflow, resulting in improper indoor air quality (Aflaki et al. 2019) and occupant

thermal discomfort (Prajongsan & Sharples 2012), especially on the leeward side of buildings (Kumar et al. 2021). Therefore, these buildings need to rely on mechanical ventilation (Tong et al. 2021), causing a large amount of energy consumption and CO_2 emissions. By opting for sustainable approachs, building designers can help reduce energy demands and minimise environmental impacts (Ahmed et al. 2021; Stasi et al. 2024). In tropical areas, where differences between indoor and outdoor air temperatures are generally not large, wind-driven cross ventilation is one of the passive design strategies recommended for maintaining indoor environmental quality at lower operating costs (Ferrucci et al. 2018; Aflaki et al. 2019; Zhang et al. 2021). It can provide higher indoor air velocity and airflow rates than single-sided ventilation (Liu et al. 2019; Park et al. 2021; Jiang et al. 2023), resulting in more efficient heat removal (Zhong et al. 2019; Stasi et al. 2024) and reducing indoor contaminants (Zhou et al. 2014). Although future trends in natural ventilation use may be constrained by climate change, it is still essential to provide this valuable option for building occupants to maintain indoor air quality in various situations and to optimise their energy costs, particularly amid Today's energy crisis (Jiang et al. 2023). Moreover, the recent COVID-19 pandemic has further highlighted the importance of fresh air in preventing indoor airborne infections (Dai & Zhao 2020; WHO 2021). Improving indoor air quality through natural ventilation can be more effective than costly mechanical ventilation, as it generally provides more fresh air (Ohba & Lun 2010; Leng et al. 2022; Muelas et al. 2022). Therefore, wind-driven cross ventilation represents a suitable method for sustainably improving the ventilation in residential buildings.

Wind-driven cross ventilation in buildings strongly depends on the design elements that allow airflow to enter from one side and exit on the opposite side by a pressure difference. However, due to the compact layout, cross ventilation can rarely be applied to double-loaded corridor configurations (Aflaki et al. 2019). Previous research has proposed several solutions to this problem, including adding extra ventilated space and designing internal openings to facilitate airflow from the windward side to the leeward side through the double-loaded corridor. The former method, such as creating wind paths (Zhou et al. 2014; Farea et al. 2015), airflow channels (Zhang et al. 2021), vertical shafts (Choi et al. 2014; Prajongsan & Sharples 2012), or air wells/ vertical voids (Seo et al. 2014; Mushin et al. 2016; Kumar et al. 2021; Laloui et al. 2021) was found to be effective in achieving cross ventilation and significantly enhance the airflow rate. However, these solutions pose drawbacks to economic feasibility due to the need for additional space, especially when applied to dense multi-family residential buildings with small dwelling units. Consequently, this study mainly focuses on improving ventilation by designing internal opening solutions that require no additional space, which are more suitable for a small unit.

Recent research on internal openings in double-loaded residential buildings has explored various design configurations. Aflaki et al. (2019) studied the dwelling unit with a transom window (TW) above the entrance door as an outlet for creating cross ventilation through double-loaded corridors in Malaysian high-rise residential buildings. The TW can increase indoor air velocity and air change rate (ACH) compared to a unit without TW, even with low outdoor wind speeds (Aflaki et al. 2019). Liu and Lee (2021) examined the unit with TW above the entrance door of high-rise residential buildings in Hong Kong. It was found that TW, serving as an outlet or inlet based on outdoor wind direction, can improve the ACH in the dwelling unit. It was also found that ACH is most sensitive to the presence of TW, followed by the position of TW to the exterior window, wind speed, area of TW, the orientation of TW, and wind direction, respectively. Tantasavasdi and Inprom (2023) investigated cross ventilation by evaluating various internal openings, including an air post, TW, and an adjustable louvre with a buffer space that allows airflow through the corridor while maintaining the occupants' privacy, listed from smallest to largest size. The findings indicate that enlarging the outlet area increases air change rates and indoor air velocities, which helps elevate the occupants' thermal comfort. Recently, Fu et al. (2024) found that adding small openings to enhance cross ventilation can be effective in both windward and leeward units of mid-rise apartment buildings across all floor levels without significantly affecting adjacent structures. Furthermore, the placement combinations of external and internal openings significantly affect airflow rates differently, depending on the floor level and wind direction.

The aforementioned studies investigate their design solutions under a limited range of wind directions, mainly perpendicular to the inlet or building. However, building orientation is often an uncontrollable factor in practice, especially on constrained urban plots. Most previous studies also lacked information on the unit's layout and the furniture inside, which significantly impacts airflow within a small space. Moreover, to our knowledge, no studies have investigated the influence of the locations of dwelling units, such as the unit at the corner compared to the middle of the building. This factor may lead to diverse ventilation performances within those units, especially in rectangular buildings that have different airflow patterns based on their shape. Therefore, this study aims to fill the research gap by investigating the improvement of wind-driven cross ventilation for small dwelling units using internal

opening solutions from previous studies, considering wind directions, unit locations, and orientations. A typical mid-rise apartment with double-loaded corridor in Bangkok, Thailand, was selected as the representative case. This study conducts field measurements to collect data for validation and performs CFD simulations to assess the ventilation performance using indoor air velocity at the occupied level and at the opening as the indices. The results are expected to be useful for decision-making in improving the natural ventilation of small dwelling units under diverse conditions.

2. Base case and design Case

A studio unit is widely adopted in Thailand, commonly found in various types of multi-residential buildings such as apartments, dormitories, condominiums, and hotels. These units typically range in size from 21 to 38 m², with 27.6 m² being the most frequently observed (Chotipanich et al, 2016). In Thailand, studio units typically characterise a narrow and elongated layout, with a width of approximately 3.8 meters. This configuration resulted from a column span of approximately 7.7 meters, which allows for three parking spaces on the ground floor. Inside the studio unit, areas for sleeping, living, dining, and food preparation are combined into a one continuous space, with bathrooms positioned adjacent to the corridor to facilitate maintenance.

Ventilation within these units is primarily limited due to a single external wall opening, as the double-loaded corridor configuration maximises unit density while maintaining an affordable price. The limited external wall and opening area result in insufficient natural ventilation, particularly in areas located further from the opening. Therefore, introducing internal openings on the entrance wall to enable cross ventilation through the corridor is an appropriate solution, as it requires no additional space and minimal maintenance. Furthermore, the studio unit layout is well-suited for incorporating buffer spaces, an approach previously proposed to maintain occupant privacy (Tantasavasdi & Inprom 2023).

Therefore, this study investigates studio units within mid-rise residential buildings, which are restricted to eight storeys or 23 metres in height under Thai building codes. These buildings represent a common typology in the urban fabric of numerous Thai provinces. Base case building is configured with a rectangular plan and a double-loaded corridor layout, where natural ventilation is provided through windows located at both ends of the corridor. The 2nd to 8th floors share an identical layout, as shown in Figure 1a. The ground floor of the building is designed as an open pilotis, accommodating parking and service areas (see Figure 1b).
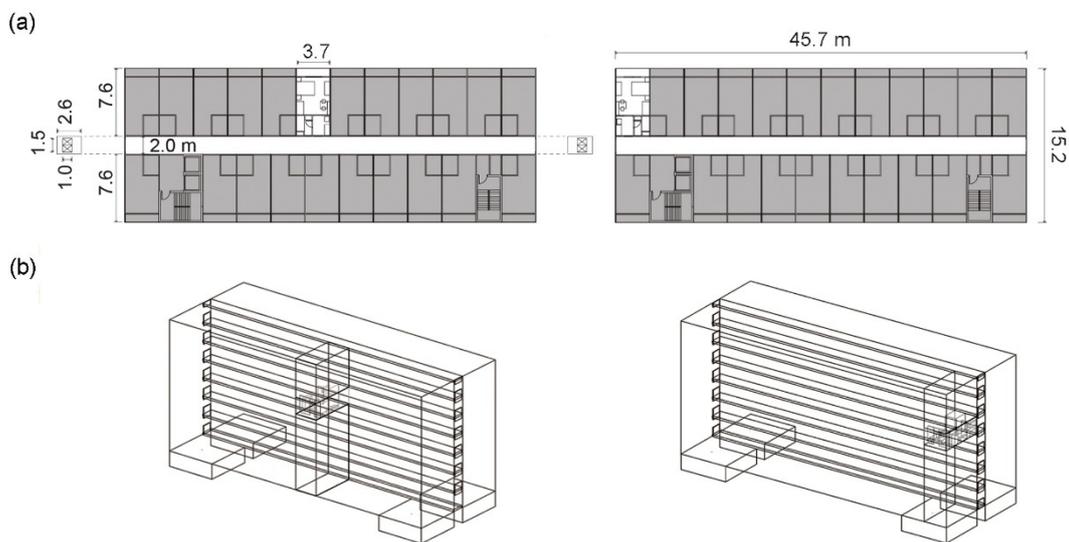

Figure 1. (a) Floor plan of the base case building, and (b) isometric view of the base case building showing the location of the middle unit and corner unit.

This study focuses on two unit locations: a corner unit and a middle unit on the 6th floor. This floor level corresponds to approximately two-thirds of the total building height and is identified as the point of most airflow stagnation (Muhsin et al. 2016; Nasrollahi & Ghobadi 2022). Both unit locations are identical in terms of size, spatial configuration, and furniture layout, but are arranged in a mirrored layout. Base case (BC) unit has a gross area of 27.4 m², with a net usable area excluding the balcony and bathroom of 19.8 m², as shown in Figure 2a. Each unit has a single sliding door sized 1.8 × 2.0 m. on the

3

external wall. As only half of this door can be utilised for ventilation, the resultant opening area is 1.8 m², resulting in an Opening-to-Floor Area Ratio (OFR) of 9.1%. The location of the opening is illustrated in Figure 2b.

The design case units in this study are improved by adding internal openings to facilitate natural ventilation through the corridor. The food preparation area within the unit is designated as a buffer space adjacent to the entrance door. This space is designed to accommodate louvre sliding doors separating it from the living area, thereby maintaining occupant privacy when the internal opening toward the corridor is used for ventilation. As the corridor-facing wall area is constrained, two design cases were explored. The first design case (C1) unit adds a 0.45 m² transom window above the entrance door (see Figure 2c), providing an OFR of 11.4%. The second (C2) unit introduces a 1.80 m² louvre door in place of the original entrance door (see Figure 2d), creating balanced area of inlet and outlet openings for better ventilation performance, with an OFR of 18.2%.
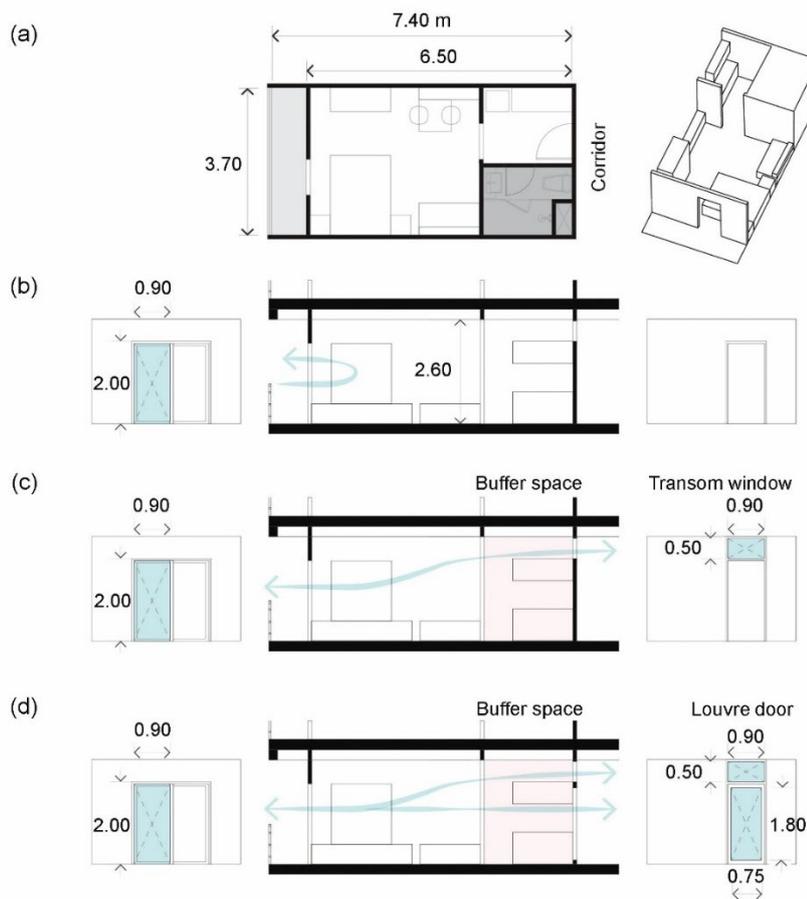

Figure 2. (a) Plan and isometric view of base case unit, elevation and section of (b) base case unit, (c) design case 1# unit, and (d) design case 2#.

3. Methods

This study uses field experiments and computational fluid dynamics (CFD) methods to investigate the ventilation performance of each unit case. This approach has been widely adopted in previous studies, as it provides results with sufficient detail and accuracy for investigating indoor wind-driven natural ventilation (Aflaki et al. 2019; Liu & Lee 2020). Field experiments of indoor air velocity were conducted in a case study building with characteristics similar to the defined base case building. The collected data were subsequently used to validate the CFD simulations for analysing ventilation performance in further different scenarios. Air velocity outputs from CFD simulations were used to analyse the impact of parameters on natural ventilation and to assess performance based on actual climatic data. The findings were summarised to propose design guidelines for enhancing natural ventilation in small dwelling units, along with recommendations for future research. The framework of this study is shown in Figure 3.
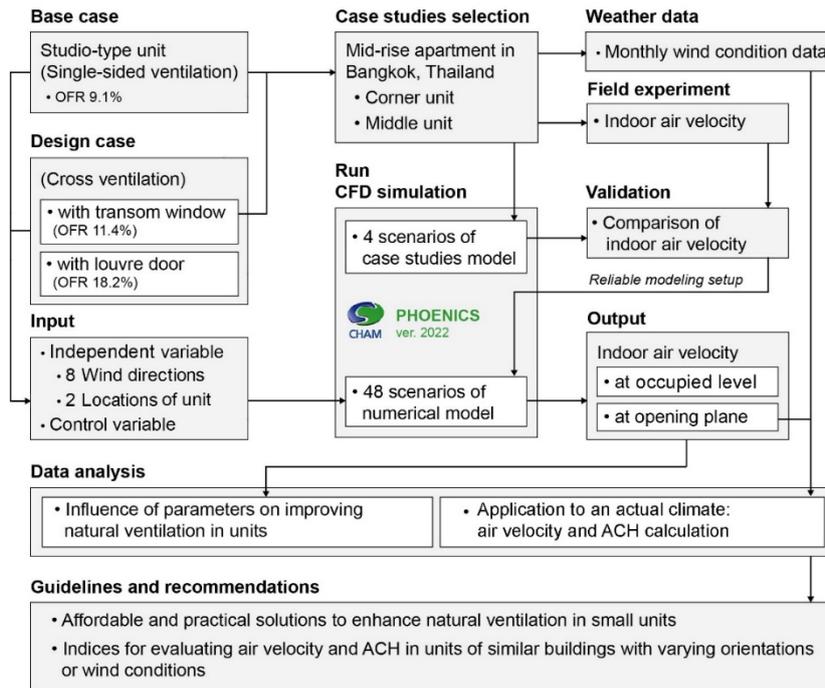
Figure 3. Research workflow.

3.1. Case study and weather data

The case study for field measurement is an eight-storey apartment building located in inner Bangkok, Thailand, under a hot and humid climate. This apartment has a floor plan similar to the BC building. The 2nd to 8th floors consist almost entirely of studio units, each with a layout similar to the BC unit but unfurnished (Figure 4a,b). The building is aligned along the NW–SE axis (Figure 4c). Within a 50-metre radius, the surrounding context contains low-rise office buildings and residential buildings, which impose minimal obstruction to wind flow (Figure 4d). This site condition is therefore considered suitable for measurements supporting CFD model validation (Liu & Lee 2020).
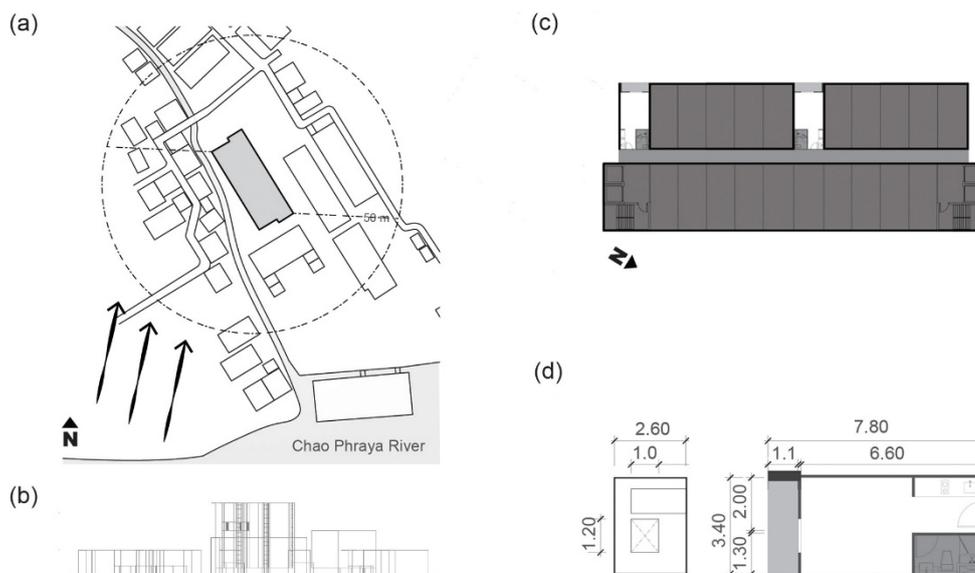

Figure 4. (a) Site plan of the case study building, (b) elevation of the case study building and surroundings, (c) floor plan of the case study building with unit location, and (d) plan and elevation of the case study unit.

The case study also represents a compact studio unit with limited ventilation located in a low-wind urban environment. Based on ten-year climatic data (2013–2022) from the nearest station (WMO 48455, Bangkok), the average outdoor wind speeds at the unit height (v_h) range from 1.31 to 1.66 m/s, with four prevailing wind directions varying monthly (Table 1). Therefore, this study measured in studio units located at the middle and corner positions on the 6th floor of the west-facing side of the building, which was the windward side during the measurement period.

Table 1. The monthly average v_h and prevailing wind direction at the location of the case study building.

Predominant wind	Month											
	Jan	**Feb**	**Mar**	**Apr**	**May**	**Jun**	**Jul**	**Aug**	**Sep**	**Oct**	**Nov**	**Dec**
Wind direction	SE	S	S	S	S	SW	SW	SW	SW	SE	NE	NE
Average v_h	1.40	1.54	1.62	1.62	1.62	1.62	1.66	1.62	1.62	1.33	1.31	1.35

3.2. Field experiments and model validation

Data collection in each case study unit was conducted under two scenarios. (1) Base case with single-sided ventilation (SV): indoor air velocity was measured in the original corner and middle unit, ventilated solely through the opening at the external wall. (2) Experimental case with cross ventilation (CV): measurements were taken in the same two units, but with cross ventilation enabled by adding an opening above the entrance door, opposite the external wall opening. The added opening, sized 0.9 × 0.2 m, was positioned 1.8 m above the floor. This was achieved by opening the entrance door and covering the lower part with a plastic sheet, while leaving the upper part to represent the added opening (see Figure 5a).

In each scenario, indoor air velocity was recorded every 2 seconds over 30 minutes at a height of 1.3 m across five measurement points (Figure 5b). For the CV cases, the measurement at the P5 position is relocated to the mid-height of the added opening (see Figure 5c). This study used a Krestel 5400 with a vane mount (accuracy: 3% of reading) set on a tripod at the balcony (Figure 5d) to measure air velocity at position P1. Testo 405i hot-wire anemometers (accuracy: ±0.1 to 0.2 m/s), also tripod-mounted, were used to measure air velocity at the external wall opening (P2) and at indoor positions P3 to P5 at the same height (Figure 5e).
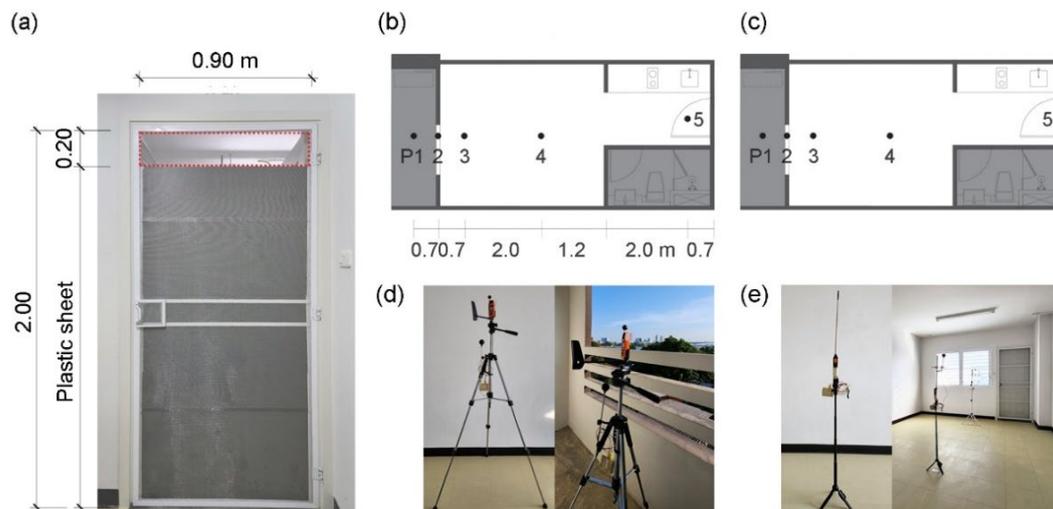

Figure 5. (a) Opening configuration in the CV case, (b) measurement points of SV case, (c) measurement points of CV case, (d) measurement instrument setup on the balcony, and (e) measurement instrument setup inside the unit.

CFD simulations were performed using PHOENICS version 2022, based on the Reynolds-averaged Navier–Stokes (RANS) equations, with a structured grid applied for air velocity analysis. The coupled approach, which simultaneously simulates the indoor and outdoor conditions, was adopted as it is suitable for modelling natural ventilation influenced by building components (Tong et al. 2016). Each CFD calculation employed the Standard K–ε model, which provides reliable predictions of air velocities in and around buildings (van Hooff et al. 2016) while offering computational efficiency (Zhao et al. 2020). The residuals of mass must be less than 0.1% for the result to be considered converged (Srebric & Chen 2002). Additionally, all the results were calculated and passed the criteria, with continuity residuals

below 0.001% and residuals of both turbulent kinetic energy (k) and turbulent kinetic energy dissipation rate (ε) below 0.1%.

The model of the case study building included surrounding buildings within a radius of twice the building height (H = 23 m) (Tominaga et al. 2008), with boundary offsets ranging from five to ten times the height, as shown in Figure 6a. The inlet boundary was defined using multiple layers with varying velocities to represent the wind profile, referencing data from the nearest meteorological station during the measurement period for each case. The model of case study building included corridor-end openings on both sides of each floor. In the case study units, no furniture was modelled, and openings were defined according to the measurement locations for both the SV case (Figure 6b) and the CV case (Figure 6c). The other units and surrounding buildings were modelled as solid objects with simplified details, and all walls were defined as solid objects with smooth-wall friction.
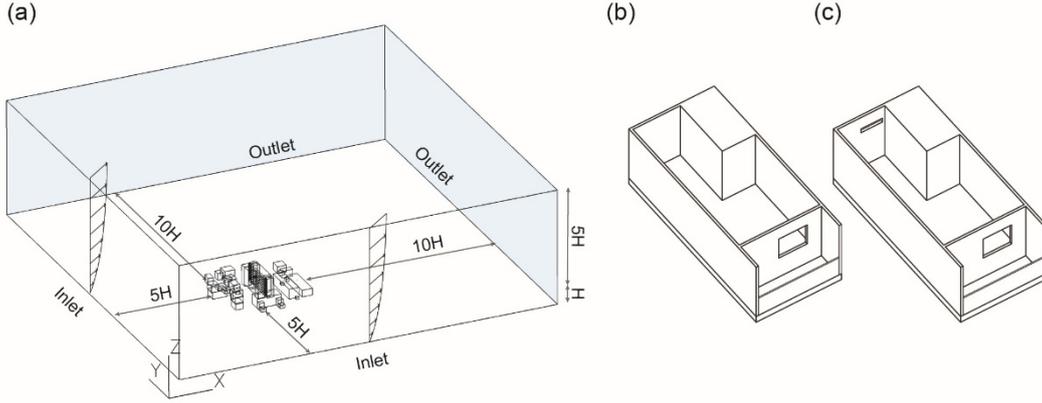

Figure 6. (a) CFD model setups showing dimensions of the domain and boundary conditions, (b) CFD model of SV case, and (c) CFD model of CV case.

This study validates the model using two statistical measures: CV(RMSE) and R², to compare the CFD simulation results with the measured data (Lee et al. 2020; Brozovsky et al. 2021). The calculations follow Equations (1) and (2), where M_i is the measured value, $\overline{M}_i$ is the mean measured value, S_i is the CFD value, and n is the total number of data points. The validation criteria are defined as CV(RMSE) less than 30% and R² more than 0.75 for the comparison of hourly wind speed measurements. The model setup that meets the specified criteria is subsequently applied to further numerical simulations.

$$CV(RMSE) = \sqrt{\frac{1}{n}\sum_{i=1}^{n}(\frac{S_i - M_i}{M_i})^2} \tag{1}$$

$$R^2 = 1 - \frac{\sum_{i=1}^{n}(M_i - S_i)^2}{\sum_{i=1}^{n}(M_i - \overline{M}_i)^2} \tag{2}$$

3.3. Numerical model scenarios and setup

This study conducted simulations of natural ventilation in the dwelling units for both the base case and the design case, comprising a total of 48 scenarios. The independent variables included three parameters: (1) opening design solutions, (2) wind directions in relation to the building orientation, and (3) locations of the unit. The dependent variables were the indoor air velocity at the occupied level and at the openings. Each scenario was governed by three sets of control variables: (1) the external environment of the residential unit, (2) the internal environment of the residential unit, and (3) the model configuration, as detailed in Table 2.

Table 2. Details of the variables used in the numerical model simulations.

Variable type	Details
Independent	1. Opening design: OFR 9.1%, OFR 11.4%, OFR 18.2%
	2. Wind direction: 0°, 45°, 90°, 135°, 180°, 225°, 270°, 315°
	3. Locations of the unit: Corner, Middle
Dependent	Indoor air velocities at the occupied level and at the opening
Control	1. External conditions of unit:
	- Including openings at the end of the corridors on each floor
	- Excluding surrounding buildings in the simulation
	- Solid adjacent rooms without any openings or façade details
	2. Internal conditions of unit:
	- Fixed unit dimensions: width, length, and height
	- Number of interior furniture items
	3. Simulation setup:
	- The boundary offset from the inlet and outlet
	- Minimum computational grid size specified
	- Turbulence model
	- Mean outdoor reference freestream velocity at unit height (v_h)

3.4. Evaluation methods

This study used the indoor air velocities obtained from CFD simulations to assess the performance of natural ventilation in each scenario. These measurements were taken at 0.5×0.5 m meshes on the horizontal plane (1.1 m above the floor). At the same time, the air velocities at the openings influence indoor air quality within the unit. These measurements were recorded at 0.3×0.3 m meshes on the vertical plane at the openings, as shown in Figure 7a.
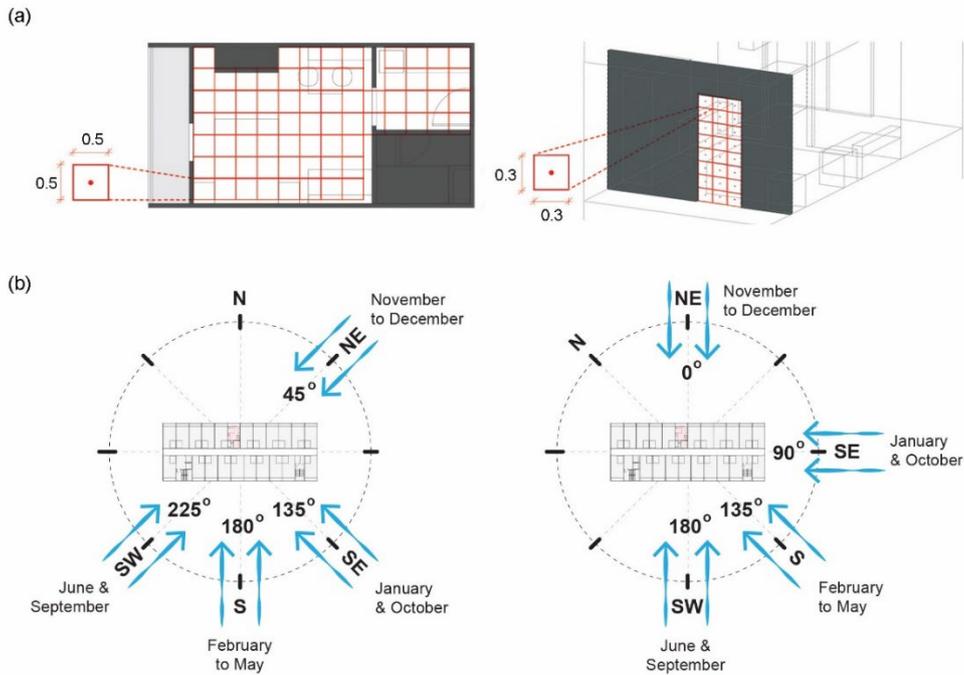

Figure 7. (a) Measurement points at the occupied level and at the openings, and (b) example application of a unit oriented towards the north (N) and northeast (NE).

Cv_i (the average velocity coefficient at the occupied level) and $Cv_o \times A$ (the product of the average

velocity coefficient at the inlet opening and the inlet opening area) were computed and further analysed in the study, as expressed in Equations (3). v_i is the indoor velocity at location i at occupied level or at opening (m/s), v_h is the mean outdoor reference freestream velocity at the unit level (m/s), n is the number of measuring meshes, and A is the inlet opening area (m²). These indices were employed to analyse the influence of the parameters on ventilation performance within the units, representing the comparison between average indoor and outdoor air velocities, and thereby offering an application for any climatic data. Figure 7b illustrates an example where we utilised values from our simulations to calculate the monthly ventilation performance within units with varying building orientations. These values, Cv_i and $Cv_o \times A$, were determined for various prevailing winds and applied across all 12 months.

$$Cv = \frac{1}{n} \times \sum_{i=1}^{n} (v_i / v_h) \tag{3}$$

$$\bar{v}_i = Cv_i \times v_h \tag{4}$$

$$ACH = \frac{3600}{V} \times (Cv_o \times A) \times v_h \tag{5}$$

Subsequently, for the application based on actual climate, the average occupied-level velocity ($\bar{v}_i$) and the air change rate (ACH) were calculated using Equations (4) and (5) to evaluated ventilation performance in each scenario. The monthly v_h is obtained from Table 1, and V is the volume of the unit (m³). The calculated $\bar{v}_i$ values at the occupied level were assessed using a minimum velocity of 0.20 m/s, as this value has been recommended to influence thermal comfort in hot and humid climatic conditions (Laloui et al. 2021). The ACH value is the most commonly used metric for ventilation efficiency, measuring the volume of air needed to replace in a space to maintain indoor air quality. This research assessed the calculated ACH values against ventilation recommendations for residential units, as shown in Table 3. It was found that most recommendations specify procedures for calculating minimum ventilation rate only for mechanically ventilated or air-conditioned spaces. For naturally ventilated spaces, the relevant requirements are found in the Thai Building Code and the U.S. CDC guidelines, which adopt different approaches. Thai Building Code specifies a minimum total opening area as a fraction of the room floor area. In contrast, U.S. CDC (2024) recommended a requirement of 5.0 ACH to reduce the risk of airborne infections in generic indoor spaces, regardless of room size. Since the base case unit already complies with the Thai Building Code regarding total opening area for natural ventilation (18%, based on a total opening area of 3.6 m² for a room area of 19.8 m²), this study adopted a 5.0 ACH criterion for indoor air quality assessment.

Table 3. The ventilation recommendation based on the base case unit.

Reference	Condition	Requirement
Thai Building Code 39 (B.E. 2537)	Natural ventilation for every room in all types of buildings.	Providing openings on the exterior wall, with a combined area ≥10% of the room area.
	Air-conditioned residential unit (Bedroom, Flow rate 0.6 l/s-m²)	0.8 ACH
	Mechanical ventilation in residential unit (Bedroom area)	7.0 ACH
ASHRAE 62.2-2022	Mechanical ventilation in residential unit (1 bedroom, area less than 47 m², Flow rate 14.0 l/s-room)	1.0 ACH
U.S. CDC 2024	Natural or mechanical ventilation to prevent COVID-19 spread in the room	5.0 ACH

4. Results

4.1. Experimental and validation results

Based on the meteorological data obtained from the nearest weather station, during the period from 6:00 to 9:00 p.m. on 5 May 2023, when measurements were conducted in the corner unit, the v_h at the unit height was recorded at 1.72 m/s. The wind direction was oblique, forming an angle of 307.5 degrees with respect to the inlet opening. During the same period on 18 May 2023, when measurements were conducted in the middle unit, the v_h was found to be 2.25 m/s, with a wind direction of 297.5 degrees relative to the inlet opening.

The measurements obtained within the middle unit under the SV scenario indicated average indoor air velocities (v_x) ranging from 0.05 to 0.75 m/s across the measurement points. Under the same SV scenario, the corner unit exhibited v_x values ranging from 0.03 to 0.69 m/s. The v_x profiles of these units under the SV scenario revealed similar trends. The highest average velocity was observed at P1 (balcony), followed by the second highest at P2 (external wall opening), with progressively lower values obtained at locations further from the opening, culminating in the lowest at P5 (corridor-side wall). The results for both units with the SV scenario are compared in terms of v_x/v_h, as presented in Figure 8. The middle unit of the SV scenario exhibited v_x/v_h values at the balcony and external wall opening slightly lower than those of the corner unit (0.07 to 0.09), while other positions showed comparable values.

Under the CV scenario, the addition of an internal opening above the entrance door increased v_x/v_h at all points compared with the SV scenarios in both unit locations (see Figure 8). The middle unit showed an increase of 0.05 to 0.70, while the corner unit showed a rise of 0.04 to 0.61. The highest ratios occurred at P5 (corridor-side opening) due to the Venturi effect caused by the smaller outlet opening, with 0.68 in the corner unit and 0.59 in the middle unit. Lower values were observed at P1, P2, and P3, respectively, while P4 consistently showed the lowest velocity in both unit locations.
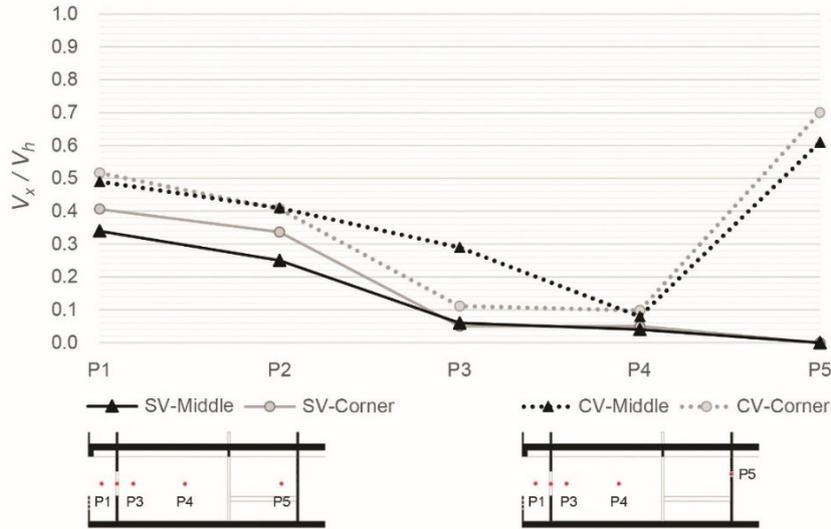

Figure 8. The v_x/v_h values at five positions obtained from the four cases.

This study tested four validation models, categorised according to their unit location and ventilation configuration, based on the field data obtained. A grid independence study was conducted with three levels of grid density, as illustrated in Figure 9: Coarse grid (349,762 cells), Basic grid (944,467 cells), and Fine grid (2,497,392 cells), using the SV–middle unit as the representative case. All three grid configurations satisfied the validation criteria, with CV(RMSE) and R^2 values within acceptable thresholds (see Table 4).

Consequently, the Basic grid configuration (CV(RMSE) = 0.19; R^2 = 0.96) was selected for the following simulations, as it provided comparable accuracy to the Fine grid while requiring approximately three times less computational time. Further validation of other cases confirmed that the modelling accuracy remained within acceptable ranges, with CV(RMSE) values between 0.16 and 0.23 and R^2 values above 0.89. Accordingly, the Basic grid configuration was adopted for all 48 numerical model scenarios in this study.

Table 4. Details of the validation models for the four unit cases.

Case	Mesh type	Smallest size	Grid number	CV(RMSE)	R^2
	Coarse	0.10m × 0.20m	349,762	0.26	0.92
SV-Middle room	Basic	0.10m × 0.10m	944,467	0.19	0.96
	Fine	0.10m × 0.05m	2,497,392	0.18	0.96
CV-Middle room	Basic	0.10m × 0.10m	998,098	0.16	0.91
SV-Corner room	Basic	0.10m × 0.10m	954,448	0.23	0.98
CV-Corner room	Basic	0.10m × 0.10m	970,904	0.21	0.89
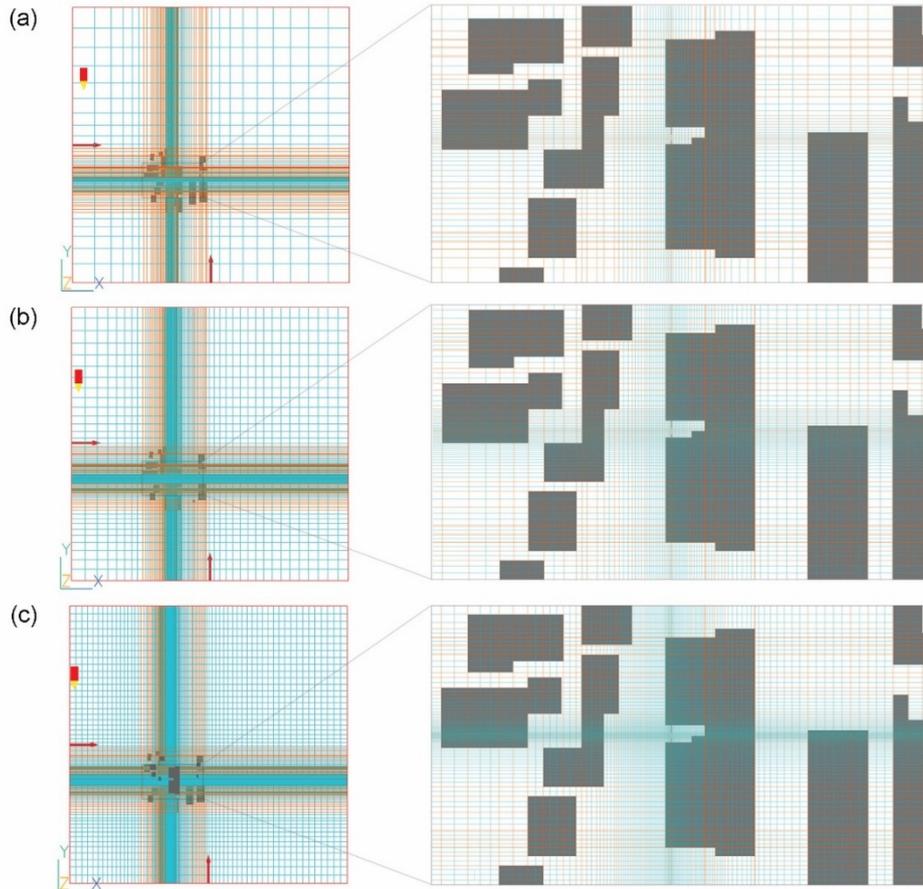
Figure 9. Three levels of grid independence study: (a) coarse grid, (b) basic grid, and (c) fine grid.

4.2. Numerical results

The simulation results of airflow around the building at the level of the represented units indicated similar patterns across all three opening design solutions. The addition of internal openings, whether in the middle or corner units, did not produce any notable differences in the airflow around the building. Differences were primarily caused by wind direction acting on the building's form, resulting in pressure variations on each façade (see Figure 10).

The extent of the stagnation zone can be categorised into three groups according to wind direction. The largest area was generated when the wind flowed perpendicularly on the long façade of the building, corresponding to wind direction in relation to building orientation of 0° or 180°. The second group comprised oblique wind directions, i.e. 45°, 135°, 225°, and 315°. The smallest stagnation zone occurred when the wind approached the short façade at 90° or 270°, allowing wind to flow directly through the corridor openings on each floor.

11

4.2.1. Base case (BC) unit

The simulation results for the base case units indicated that higher indoor air velocities occurred at the occupied level only in the balcony area and the immediate vicinity of the opening (Figure 11a). At the same time, the more deeply occupied zones within the units exhibited low consistency in air velocities across the entire area. This trend was consistent for all BC scenarios, regardless of unit location or wind direction. Table 5 presents the Cv_i values of all BC scenarios at the middle and corner location, which were found to be very low and nearly identical across all eight wind directions (average $Cv_i = 0.01$ and 0.02, respectively). By comparison, the $Cv_o \times A$ values are consistently low, varying with wind direction from 0.01 to 0.04 for the middle unit and from 0.00 to 0.05 for the corner unit.
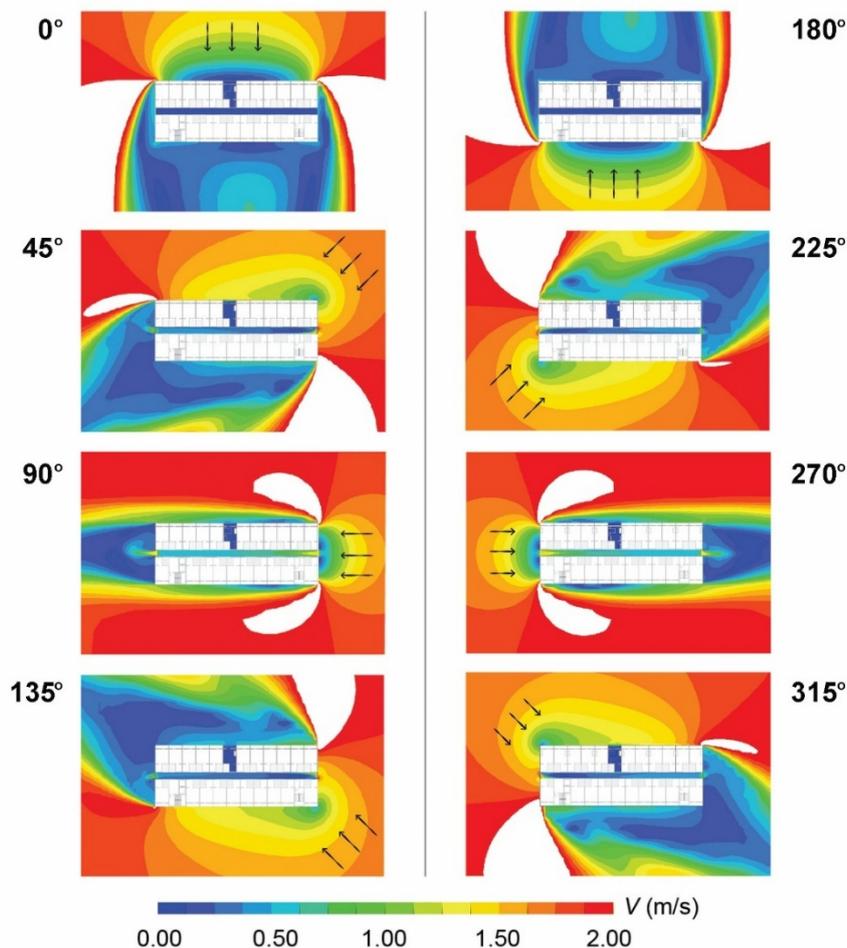

Figure 10. Simulation results of airflow around the building at the represented unit level under eight wind directions.

4.2.2. Case 1 (C1): Unit with transom window

Introducing a transom window to enable cross ventilation within the units (Figure 11b) substantially improved airflow distribution compared with the BC scenarios. Two airflow sources could be identified: (1) under wind directions of 0°, 45°, 180°, and 315°, airflow entered through the external wall opening, and (2) under wind directions of 90°, 135°, 225°, and 270°, airflow entered through the transom window above the entrance door. In windward units, particularly at 0°, significant velocity increases were generated in the occupied area aligned with the openings. In contrast, leeward units, under wind directions such as 135° and 180°, experienced large stagnation areas, resulting in low indoor velocities similar to those of the BC units.

Moreover, the results found that mean air velocities at the transom opening are higher than those at the external wall opening, due to the Venturi effect induced by its smaller effective area. As shown in Table 5, the Cv_i and $Cv_o \times A$ values for C1 scenarios were slightly higher in the middle unit (0.05–0.15

and 0.11–0.47, respectively) than in the corner unit (0.04–0.15 and 0.10–0.43). The highest Cv_i and Cv_o $\times$ A values occurred under the 0° wind direction, while the lowest were found under the 180° wind direction, consistent across both unit locations.

4.2.3. Case 2 (C2): Unit with louvre door

The simulation of the improved case, which added a louvre door for cross ventilation (Figure 11c), revealed airflow characteristics similar to those of C1 units, with two sources of incoming air depending on the wind direction. The larger opening size facilitated greater airflow penetration under all wind conditions, with the high-velocity zones (lighter colours) extending beyond the areas directly aligned with the openings into wider portions of the occupied area compared with the previous case. As presented in Table 5, the Cv_i and Cv_o $\times$ A values for the middle unit ranged from 0.05–0.15 and 0.11–0.47, respectively, slightly higher than those of the corner unit (0.04–0.15 and 0.10–0.43). The 0° wind direction continued to produce the highest Cv_i and Cv_o $\times$ A values, while the 180° wind direction generated the lowest, consistent for both middle and corner units.
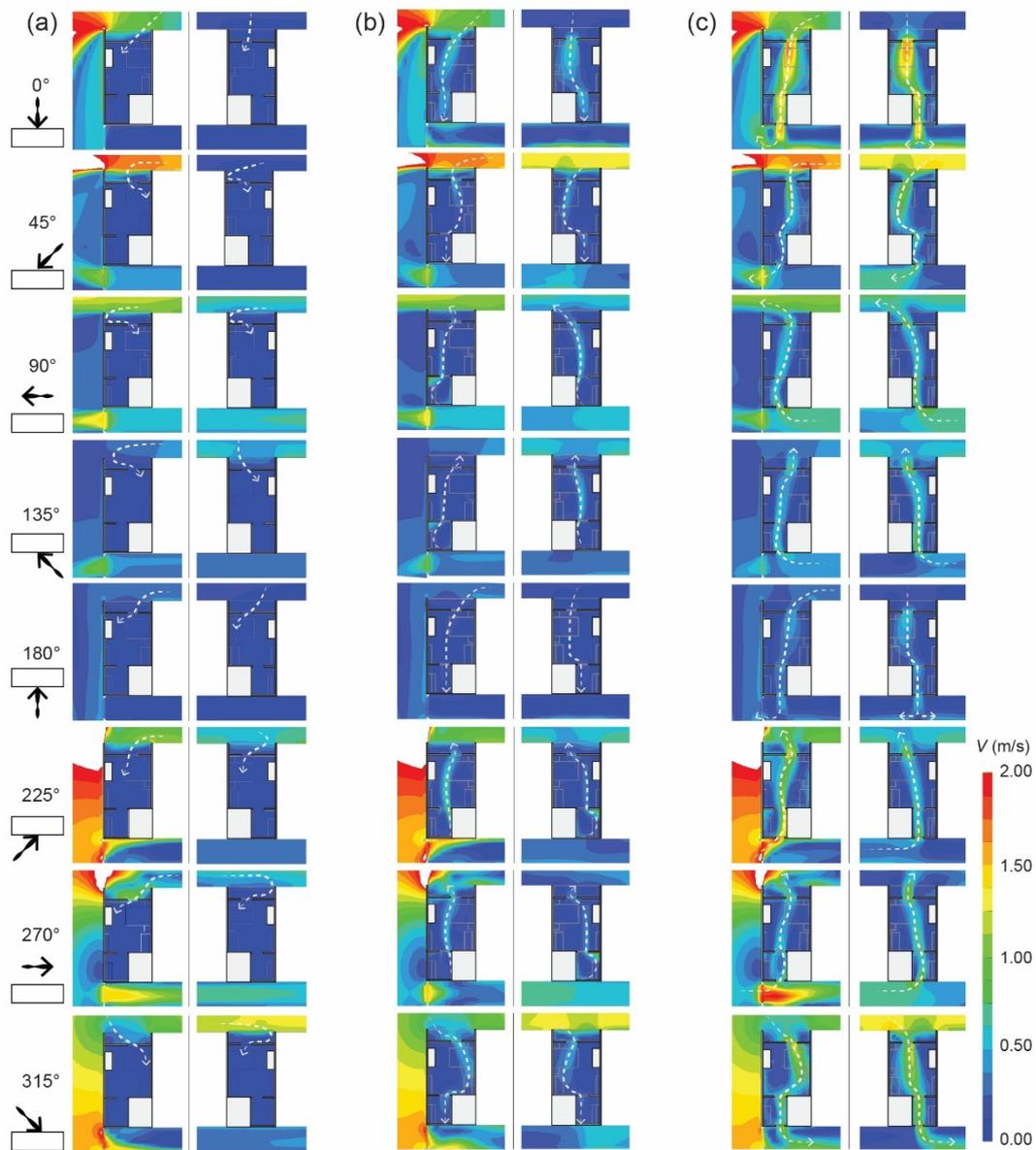

Figure 11. Airflow simulation at the occupied level: corner unit (right) and middle unit (left) for (a) BC, (b) C1, and (c) C2 scenarios.

13

Table 5. Cv_i and $Cv_o \times A$ values across all 48 scenarios.

Wind direction	Case	Cv_i		$Cv_o \times A$	
		Middle	**Corner**	**Middle**	**Corner**
0°	Base case	0.01	0.02	0.01	0.03
	Case 1	0.15	0.15	0.47	0.43
	Case 2	0.38	0.39	1.34	1.33
45°	Base case	0.01	0.02	0.03	0.05
	Case 1	0.09	0.07	0.29	0.19
	Case 2	0.21	0.14	0.77	0.45
90°	Base case	0.01	0.01	0.02	0.04
	Case 1	0.09	0.08	0.25	0.25
	Case 2	0.17	0.15	0.66	0.64
135°	Base case	0.01	0.01	0.03	0.01
	Case 1	0.09	0.06	0.22	0.16
	Case 2	0.17	0.13	0.69	0.54
180°	Base case	0.01	0.01	0.00	0.01
	Case 1	0.05	0.04	0.11	0.10
	Case 2	0.13	0.12	0.50	0.43
225°	Base case	0.01	0.02	0.04	0.05
	Case 1	0.08	0.12	0.23	0.30
	Case 2	0.16	0.26	0.75	1.03
270°	Base case	0.01	0.02	0.03	0.03
	Case 1	0.09	0.11	0.25	0.27
	Case 2	0.17	0.15	0.71	0.61
315°	Base case	0.01	0.01	0.01	0.01
	Case 1	0.09	0.10	0.31	0.39
	Case 2	0.28	0.26	0.85	0.94

5. Discussion

5.1. Influence of design parameters

Figure 12 presents the box plots of Cv_i and $Cv_o \times A$ values, representing the indices of ventilation performance across all 48 scenarios, categorised by opening design, wind direction, and unit location. Analysis of changes in mean values revealed that the opening design had the most significant influence on both indices, with mean Cv_i and mean $Cv_o \times A$ increasing by factors of 15.5 and 32.0, respectively, when transitioning from the BC to the C2 case. Wind direction in relation to building orientation was the second most influential parameter, which resulted in maximum increases of 3.1 times for mean Cv_i and 3.2 times for mean $Cv_o \times A$ when changing from the 180° to 0° case. Unit location, on the other hand, had the least effect, with mean Cv_i and mean $Cv_o \times A$ increasing by less than 1.1 times. The detailed trends of Cv_i and $Cv_o \times A$ for each parameter are explained as follows.
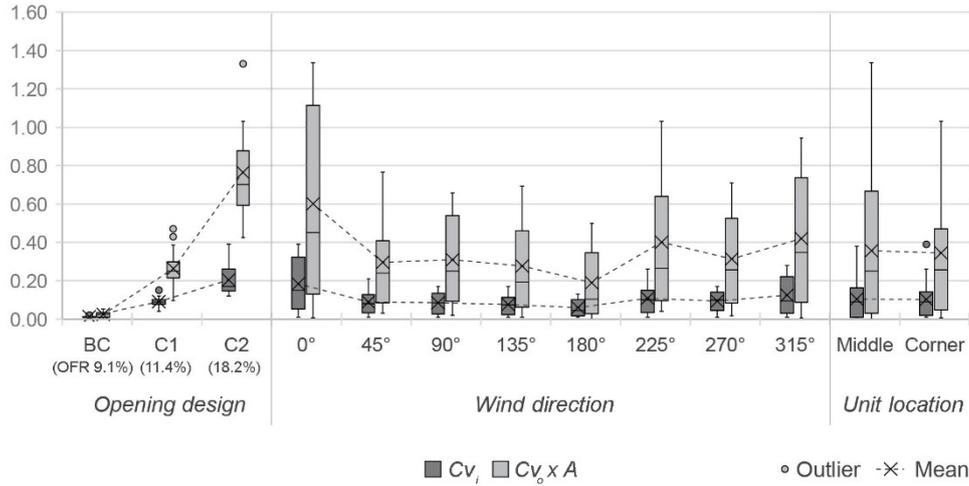
Figure 12. Box plots of Cv_i and $Cv_o \times A$ values across all 48 scenarios.

5.1.1. Opening design

The comparative analysis between the opening design approaches of the BC unit with 16 scenarios, C1 unit with 16 scenarios, and C2 unit with 16 scenarios indicates that improvements in opening design, reflected in higher OFR values, consistently lead to corresponding increases in both Cv_i and $Cv_o \times A$ within dwelling units. This trend is evident across all scenarios, as illustrated in Figure 13.
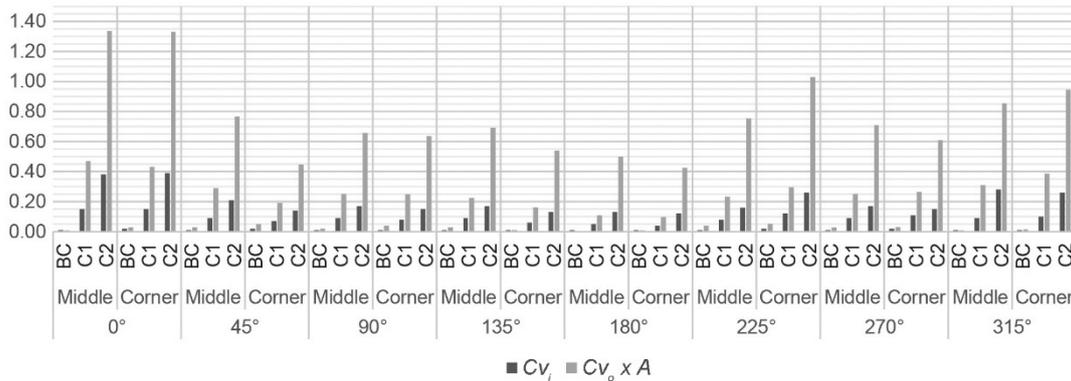

Figure 13. Bar chart of Cv_i and $Cv_o \times A$ values across different opening design parameters.

The improvement from the BC unit, with single-sided ventilation, to the C1 unit with a transom window enabling cross ventilation, resulted in substantial improvements in indoor ventilation performance, with Cv_i and $Cv_o \times A$ values increasing by factors of 3.5 to 15.0 and 3.8 to 110.0, respectively. Similarly, the transition from the BC unit to the C2 unit, which adopted a louvre door to promote cross ventilation, resulted in greater enhancements, with Cv_i and $Cv_o \times A$ values increasing by factors of 7.0 to 38.0 and 8.9 to 499.0, respectively. These findings are consistent with previous studies, which have found that dwelling units with cross ventilation perform several times better than those with single-sided ventilation (Aflaki et al. 2019; Liu & Lee 2020; Tantasavasdi & Inprom 2023; Lin et al. 2025), despite a minor increase in OFR (2.3% from BC to C1). Furthermore, cross ventilation can also improve ventilation performance even when the units are located on the leeward side (Fu et al. 2024).

The change of the design approach from C1 unit to C2 unit, which had an increased opening area (with OFR rising by 6.8%), indicated that the improvement through larger openings and equal inlet-to-outlet ratios resulted in higher Cv_i and $Cv_o \times A$ values in all scenarios, with increases ranging from 1.4 to 3.1 times and 2.3 to 4.5 times, respectively. These results align with previous research, which demonstrates that increased opening areas significantly influence indoor ventilation rates (Sacht & Lukiantchuki 2017; Liu & Lee 2020) and further contribute to enhancing air velocity at the occupied

level (Tantasavasdi & Inprom 2023).

5.1.2. Wind direction in relation to building orientation

The comparative analysis of 8 wind directions in relation to building orientation across 6 scenarios (see Figure 14) indicates that the Cv_i and $Cv_o \times A$ values of the unit varied according to the ventilation configurations. For the BC units with single-sided ventilation, variations in wind direction exerted minimal influence on Cv_i values (less than 0.01). Notably, in the unit located in the middle of the building, wind direction had no discernible effect on Cv_i values. In contrast, the impacts of changes in wind direction on the $Cv_o \times A$ values were found to vary, ranging from 1.3 to 5.0 times. In the cases of cross-ventilated units (C1 and C2), variations in wind direction resulted in changes to Cv_i and $Cv_o \times A$ values, ranging from 1.3 to 3.8 times and 1.1 to 4.4 times, respectively.
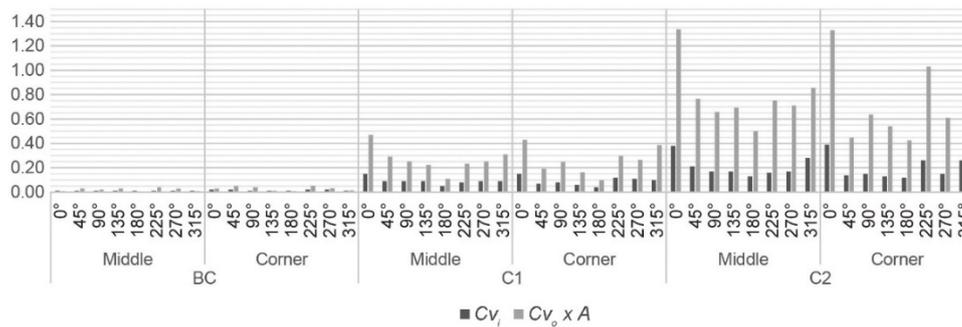

Figure 14. Bar chart of Cv_i and $Cv_o \times A$ values across different wind direction parameters.

This study found that the 0° case, where wind acts perpendicular to the building façade, provided the best Cv_i and $Cv_o \times A$ values for cross ventilation units, in line with previous findings (Jiang et al. 2023; Miše et al. 2024). Conversely, in single-sided ventilated units, oblique or parallel wind directions relative to the openings were found to facilitate more effective ventilation than perpendicular airflow (Miše et al. 2024; Stenech et al. 2025).

For the cross ventilation units (C1 and C2), greater deviations of wind direction from perpendicular openings resulted in reductions of both Cv_i and $Cv_o \times A$ relative to the 0° case, with variations depending on the location of the unit. In the middle unit, oblique windward incidences (45°, 315°) reduced Cv_i and $Cv_o \times A$ by 1.7 to 1.9 and 1.5 to 1.7, respectively. These are followed by parallel winds (90°, 270°) and oblique leeward flows (135°, 225°), which produce larger decreases of 2.2 to 2.4 and 1.8 to 2.1, respectively.

In the corner unit, oblique windward flows (225°, 315°) resulted in reductions of 1.2 to 1.5 and 1.1 to 1.5 for Cv_i and $Cv_o \times A$, respectively. Parallel winds (90°, 270°) showed greater decreases of 1.5 to 2.6 and 1.6 to 2.2, while oblique downstream or leeward wind (45°, 135°) produced even more substantial reductions of 2.1 to 3.0 and 2.3 to 3.0, respectively. Finally, the 180° case consistently exhibited the poorest performance across both the middle and corner units, with reductions of 2.9 to 3.8 and 2.7 to 4.4, respectively, due to the units being positioned directly opposite the incoming wind.

5.1.3. Location of unit

The comparative analysis of Cv_i and $Cv_o \times A$ values between 24 scenarios of middle units and 24 scenarios of corner units, as shown in Figure 15, revealed differing trends depending on the ventilation type of the units, similar to the trends of wind direction parameters.
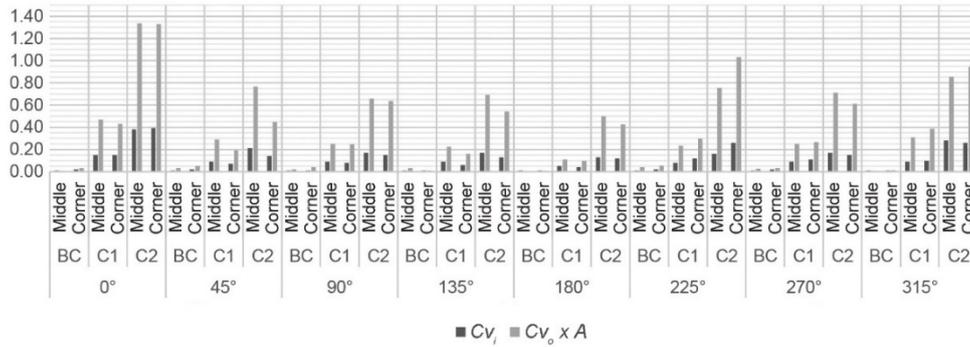
Figure 15. Bar chart of Cv_i and $Cv_o \times A$ values across different unit location parameters.

For BC units with single-sided ventilation, unit location had minimal impact on Cv_i values (less than 0.01). However, in corner units, most scenarios (7 out of 8) demonstrated $Cv_o \times A$ values between 1.1 and 7.0 times greater than those of the middle unit. For cross-ventilated rooms (C1 and C2), variations in unit location exerted minimal influence on Cv_i and $Cv_o \times A$ values (less than 0.02) under wind directions of 0° and 90°. For different wind directions, it was observed that the location of units had varying effects on the Cv_i and $Cv_o \times A$ values. These effects ranged from 1.1 to 1.6 times for Cv_i and from 1.1 to 1.7 times for $Cv_o \times A$. The trends differed depending on whether the unit was situated on the windward or leeward side.

Figure 16 compares two locations of the unit under identical wind incidence angles. When the wind approached the building at 45° (Figure 16a), the middle unit functioned as the windward side, with airflow through the opening at a more oblique angle relative to the corner unit, located at the downstream side of the airflow (Figure 16b). At the downstream side, wind direction tended to align more parallel with the opening of the unit due to wind deflection along the large building façade. Therefore, the probability of airflow entering the downstream unit was lower than that of the windward unit. As a result, Cv_i and $Cv_o \times A$ values in downstream unit were consistently lower than those in windward unit.
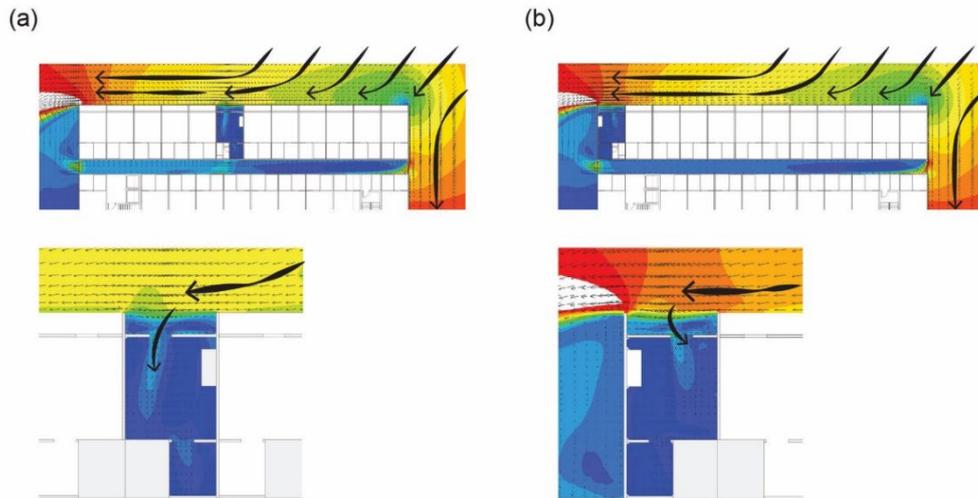

Figure 16. Airflow patterns around (a) a middle unit on the windward side, and (b) a corner unit on the downstream side under wind direction at 45° to the building.

5.2. Application to an actual climate

In this study, Cv_i and $Cv_o \times A$ were integrated with v_h and wind direction data from Bangkok's weather (Table 1) to evaluate air velocity at the occupied level and the ACH, providing a basis to assess the natural ventilation performance of each unit. The calculated air velocity at the occupied level for all 12 months, across each unit location with eight different orientations, is summarised in Figure 17. The findings reveal that BC units demonstrated extremely low air velocities at the occupied level (0.01–0.04 m/s), uniformly across both middle and corner locations. In all scenarios of the BC unit, the measured

17

values were substantially below the recommended criterion for enhancing thermal comfort.

In C1 units, although occupied-level air velocities were considerably higher than in BC units, they remained low in most scenarios, with only specific periods exceeding the recommended criterion of 0.2 m/s. These variations were influenced by building orientation and unit location. Specifically, middle C1 units facing NE, S, and SW, and corner C1 units facing N, S, SW, and NW, were able to achieve the criterion due to their exposure to prevailing windward flows during certain periods. At the same time, the C2 units occupied-level air velocities met the recommendation in nearly all scenarios throughout the 12 months (with Cv_i values ≥ 0.15), resulting in airflow velocities between 0.20 and 0.65 m/s. Exceptions occurred in middle C2 units facing SW and NW, and in corner C2 units facing N, SW, W, and NW, where air velocities occasionally dropped below the criterion due to periodic exposure to prevailing leeward winds.

The monthly calculated ACH values for each unit across different building orientations varied considerably, ranging from 0.1 to 169.5 in middle units (Figure 18a) and from 0.7 to 168.7 in corner units (Figure 18b). Based on the minimum ventilation requirement in this study in Table 3 (ACH $\geqslant 5.0$), it was found that BC unit scenarios (ACH = 0.1 to 6.6) barely met the criterion. In contrast, all the proposed units—C1 (ACH = 9.7 – 59.6) and C2 (ACH = 42.5 – 169.5)—met the criterion across all orientations throughout the year, regardless of the unit's location. These findings indicate that the proposed solutions for cross ventilation (C1 and especially C2 units) substantially enhance natural ventilation compared to single-sided ventilation (BC units). The results also confirm that such solutions are applicable across all eight building orientations, offering strategies for improving both thermal comfort and indoor air quality in residential buildings within hot and humid climates.
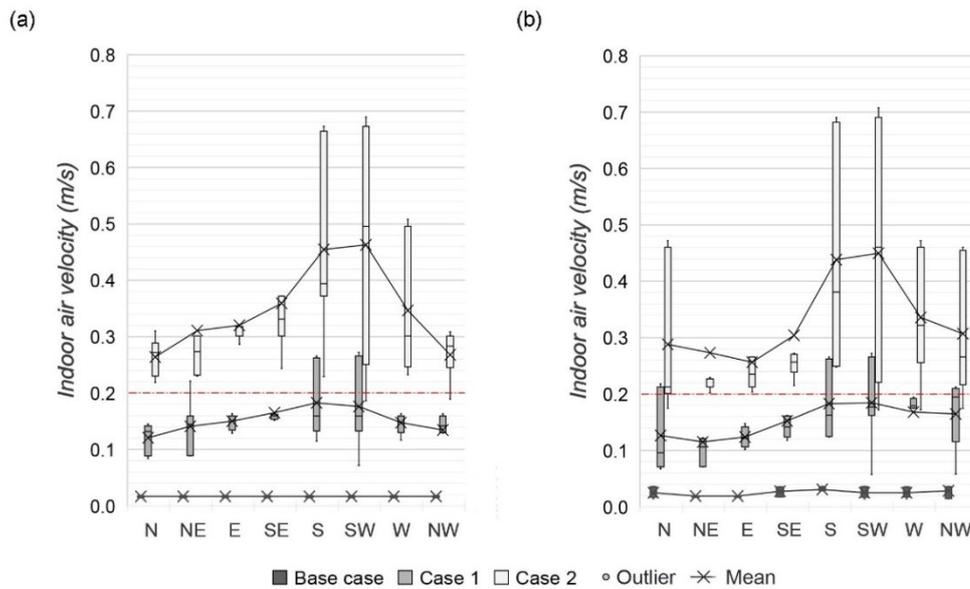

Figure 17. Box plots presenting the annual average occupied-level air velocity within units, comparing (a) the middle units, and (b) the corner units across different building orientations.
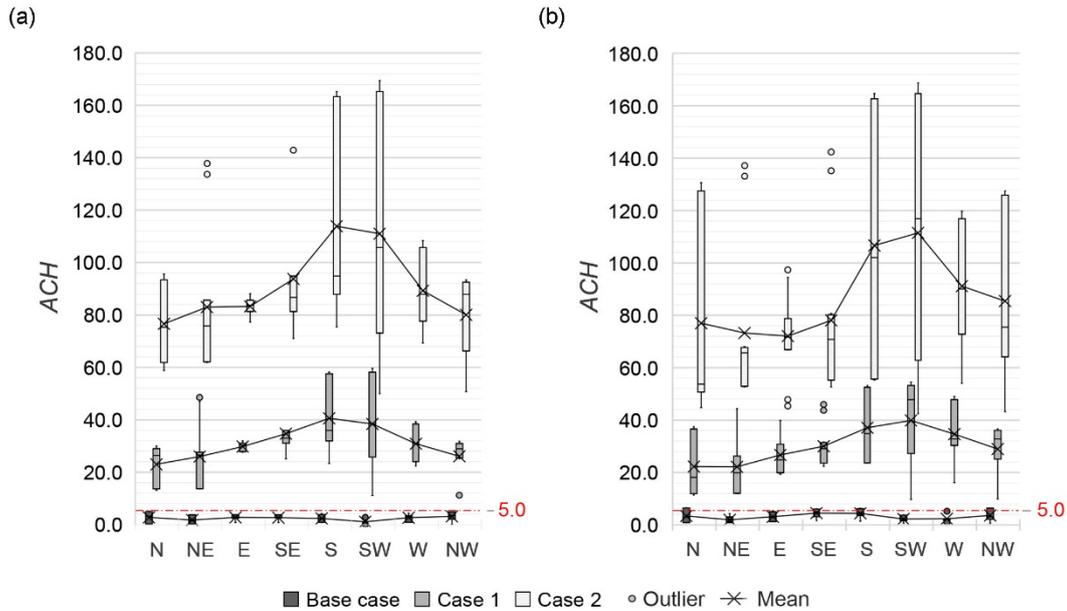
Figure 18. Box plots presenting the annual ACH values within units, comparing (a) the middle units, and (b) the corner units across different building orientations.

5.3. Limitations

This study is subject to certain limitations, particularly in the numerical simulation, as the influence of surrounding buildings and obstructions at the openings (e.g., louvres or insect screens) was not considered. The simulations were limited to a representative single floor level, whereas units located at other levels may exhibit different ventilation behaviours. Moreover, the evaluation in this study focused solely on wind speed as perceived by occupants, without incorporating other factors, such as air temperature and relative humidity, that affect overall thermal comfort.

Future investigations could therefore adopt more comprehensive simulation scenarios, including the aforementioned variable, to yield more practically relevant findings. The design solutions proposed in this study should also be applied with caution, taking into account the building type and user profile, as the implications for acoustic privacy were beyond the scope of this study.

6. Conclusion

This study examines solutions to enhance natural ventilation in small dwelling units within mid-rise, double-loaded corridor buildings, where single-sided ventilation is often insufficient. The base case was a compact studio-layout unit (OFR 9.1%), representative of common unit in Thailand. Two cross ventilation solutions were proposed: adding a buffer space at the entrance with either a transom window (OFR 11.4%) or a louvre door (OFR 18.2%), enabling airflow through the naturally ventilated corridor. Field measurements combined with CFD simulations, validated against observed data, confirmed the reliability of the modelling approach. Air velocities measured at the occupied level and at the internal openings were employed to calculate Cv_i and $Cv_o \times A$ as the indices for performance evaluation. The main results are summarised below:

- The BC units with single-sided ventilation performed poorly in all scenarios, with Cv_i values ranging from 0.01 to 0.02 and $Cv_o \times A$ values from 0.01 to 0.05. In comparison, the C1 unit (transom window) improved Cv_i and $Cv_o \times A$ up to 15.0 and 110.0 times, while the C2 unit (louvre door) achieved increases of up to 38.0 and 499.0 times, respectively.
- The opening design had the most significant impact on average Cv_i and $Cv_o \times A$, with both indices tending to rise in line with higher OFR values, consistent with previous studies. The next most significant parameter was the wind direction in relation to building orientation, followed by the location of the unit.
- Based on the application using Bangkok weather data, BC units exhibited low air velocities and frequently failed to meet the ACH requirement, particularly in the middle units. By contrast, C1 units consistently met the requirement regardless of location, despite low indoor air velocities. At the same

19

time, C2 units not only satisfied the ACH requirement across all scenarios but also achieved higher air velocities, contributing to improved thermal comfort.

- For both new building designs and retrofit projects aiming to enhance indoor air quality, the adoption of the C1 solution is generally sufficient. When higher air velocities are required to enhance thermal comfort or reduce reliance on mechanical systems, the C2 solution is more suitable, although with lower privacy compared to the C1 solution.
- In cases where only smaller openings can be introduced while facing face low wind velocities or unfavourable wind directions, future research on alternative solutions should be considered, such as adopting special façade configurations or providing additional openings in corridors.

The Cv_i and $Cv_o \times A$ values in this study can be applied to evaluate the ventilation performance of similar dwelling units under other climatic conditions. The findings reveal both the potential and limitations of introducing internal openings for cross ventilation in compact units across various wind directions and locations. Designing residential units with effective natural ventilation strategies should therefore be regarded as a critical concern for both architects and policymakers. Future improvements should further address additional impacts beyond the limitations of this study to support sustainable residential building development while enhancing living quality.

References
Aflaki, A, Hirbodi, K, Mahyuddin, N, Yaghoubi, M and Esfandiari, M. 2019. Improving the air change rate in high-rise buildings through a transom ventilation panel: A case study. Building and Environment, 147: 35–49. DOI: https://doi.org/10.1016/j.buildenv.2018.10.011

Ahmed, T, Kumar, P and Mottet, L. 2021. Natural ventilation in warm climates: The challenges of thermal comfort, heatwave resilience and indoor air quality. Renewable and Sustainable Energy Reviews, 138: 110669. DOI: https://doi.org/10.1016/j.rser.2020.110669

ASHRAE (American Society of Heating, Refrigerating and Air-Conditioning Engineers) 2022 ANSI/ASHRAE Standard 62.2-2022: Ventilation for Acceptable Indoor Air Quality in Residential Buildings. Atlanta, GA: ASHRAE.

Brozovsky, J, Simonsen, A and Gaitani, N. 2021. Validation of a CFD model for the evaluation of urban microclimate at high latitudes: A case study in Trondheim, Norway. Building and Environment, 205: 108175. DOI: https://doi.org/10.1016/j.buildenv.2021.108175

Choi, J, Choi, Y, Kim, Y and Kang, J. 2014. Apartment prototype with enhanced natural ventilation system for Vietnam. Journal of Asian Architecture and Building Engineering, 13(2): 303–308. DOI: https://doi.org/10.3130/jaabe.13.303

Chotipanich, S, Povatong, B and Jenjapoo, T. 2016. The relationship between the unit size and price of studio-type condominium in Bangkok metropolitan area. Academic Journal of Architecture, 65: 99-110. DOI: https://so01.tci-thaijo.org/index.php/AJA/article/view/164400.

Dai, H and Zhao, B. 2020. Association of the infection probability of COVID-19 with ventilation rates in confined spaces. Building Simulation, 13: 1321-1327. DOI: https://doi.org/10.1007/s12273-020-0703-5

Farea, TG, Ossen, DR, Alkaff, S and Kotani, H. 2015. CFD modeling for natural ventilation in a lightwell connected to outdoor through horizontal voids. Energy and Buildings, 86: 502-513. DOI: https://doi.org/10.1016/j.enbuild.2014.10.030

Ferrucci, M, Brocato, M and Peron, F. 2018. Digital tools for the morphological design of the naturally ventilated buildings. Future Cities and Environment, 4(1): 1–9, DOI: https://doi.org/10.5334/fce.4

Fu, X, Tai, V, Moey, L, Rahman, N, Ahmad, K and Baglee, D. 2024. Opening configurations and natural cross ventilation performance in a double-loaded multi-level apartment building: A CFD analysis. Building and Environment, 254: 111404. DOI: https://doi.org/10.1016/j.buildenv.2024.111404.

Jiang, Z, Kobayashi, T, Yamanaka, T and Sandberg, M. 2023. A literature review of cross ventilation in buildings. Energy & Buildings, 291: 113143. DOI: https://doi.org/10.1016/j.enbuild.2023.113143

Kumar, N, Kubota, T, Tominaga, Y, Shirzadi, M and Bardhan, R. 2021. CFD simulations of wind-induced ventilation in apartment buildings with vertical voids: Effects of pilotis and wind fin on ventilation performance. Building and Environment, 194: 107666. DOI: https://doi.org/10.1016/j.buildenv.2021.107666

Laloui, H, Majid, NHA and Sanusi, ANZ. 2021. A numerical investigation on the impacts of voids combinations on natural ventilation of high-rise residential building. Open House International, 46(2): 304-324. DOI: https://doi.org/10.1108/OHI-11-2020-0157

Lee, M, Park, G, Park, C and Kim, C. 2020. Improvement of grid independence test for computational fluid dynamics model of building based on grid resolution. Advances in Civil Engineering, 8827936. DOI: https://doi.org/10.1155/2020/8827936

Leng, PC, Aw, SB, Ali, NEH, Ling, GHT, Lee, YL and Ahmad, MH. 2022. Solar chimneys as an effective ventilation strategy in multi-storey public housing in the post-COVID-19 era. Buildings, 12: 820. DOI: https://doi.org/10.3390/buildings12060820

Lin, P, Qin, H, Lau, S and Wei, Q. 2025. Impact of unit type and configuration on indoor natural ventilation performance of high-rise, high-density residential buildings in Hong Kong. Building and Environment, 269: 112444. DOI: https://doi.org/10.1016/j.buildenv.2024.112444

Liu, T and Lee, WL. 2020. Evaluating the influence of transom window designs on natural ventilation in high-rise residential buildings in Hong Kong. Sustainable Cities and Society, 62: 102406. DOI: https://doi.org/10.1016/j.scs.2020.102406

Liu, S, Pan, W, Cao, Q, Long, Z, Jiang, Y and Chen, Q. 2019. CFD simulations of natural cross ventilation through an apartment with modified hourly wind information from a meteorological station. Energy and Buildings, 195: 16-25. DOI: https://doi.org/10.1016/j.enbuild.2019.04.043

Miše, D, Irrenfried, C, Meile, W, Brenn, G and Kozmar, H. 2024. Wind-driven natural ventilation of cubic buildings in rural and suburban areas. Journal of Building Engineering, 87: 10874. DOI: https://doi.org/10.1016/j.jobe.2024.108740

Muelas, A, Remacha, P, Pina, A, Tizné, E, El-Kadmiri, S, Ruiz, A, Aranda, D and Ballester, J. 2022. Analysis of different ventilation strategies and CO2 distribution in a naturally ventilated classroom. Atmospheric Environment, 283: 119176. DOI: https://doi.org/10.1016/j.atmosenv.2022.119176.

Muhsin, F, Yusoff, WFM, Mohamed, MF and Sapian, AR. 2016. The effects of void on natural ventilation performance in multi-storey housing. Buildings, 6(3): 35. DOI: https://doi.org/10.3390/buildings6030035

Nasrollahi, N and Ghobadi, P. 2022. Field measurement and numerical investigation of natural cross-ventilation in high-rise buildings; Thermal comfort analysis. Applied Thermal Engineering, 211: 118500. DOI: https://doi.org/10.1016/j.applthermaleng.2022.118500

Ohba, M and Lun, I. 2010. Overview of natural cross-ventilation studies and the latest simulation design tools used in building ventilation-related research. Advances in Building Energy Research, 4(1): 127–166. DOI: https://doi.org/10.3763/aber.2009.0405

Peters, T and Halleran, A. 2021. How our homes impact our health: Using a COVID-19 informed approach to examine urban apartment housing. Archnet-IJAR, 15(1): 10–27. DOI: https://doi.org/10.1108/ARCH-08-2020-0159

Prajongsan, P and Sharples, S. 2012. Enhancing natural ventilation, thermal comfort and energy savings in high-rise residential buildings in Bangkok through the use of ventilation shafts. Building and Environment, 50: 104–113. DOI: https://doi.org/10.1016/j.buildenv.2011.10.020

Sacht, H and Lukiantchuki, M. 2017. Windows size and the performance of natural ventilation. Procedia Engineering, 196: 972-979. DOI: 10.1016/j.proeng.2017.08.038.

Seo, R, Lee, L and Jeon, S. 2014. The typologies of block and unit plan in Malaysian apartments - focused on middle cost houses supplied by the private sector. Journal of Asian Architecture and Building Engineering, 13(2): 397–404. DOI: https://doi.org/10.3130/jaabe.13.397

Sha, H and Qi, D. 2020. A Review of high-rise ventilation for energy efficiency and safety. Sustainable Cities and Society, 54: 101971. DOI: https://doi.org/10.1016/j.scs.2019.101971

Srebric, J and Chen, Q. 2002. An example of verification, validation, and reporting of indoor environment CFD analyses. ASHRAE Transactions, 108(2): 185-194.

Stasi, R, Ruggiero, F and Berardi, U. 2024. Influence of cross-ventilation cooling potential on thermal comfort in high-rise buildings in a hot and humid climate. Building and Environment, 248: 111096. DOI: https://doi.org/10.1016/j.buildenv.2023.111096

Stenech, M, Decitre, G, Brenn, G and Irrenfried, C. 2025. Experimental investigation of the ventilation efficiency for single-sided ventilation in suburban areas. Building and Environment, 283: 113280. DOI: https://doi.org/10.1016/j.buildenv.2025.113280

Tantasavasdi, C and Inprom, N. 2023. Residential unit design for natural ventilation in tropical multi-family high-rises with a double-loaded corridor. Nakhara: Journal of Environmental Design and Planning, 22(3): Article 315. DOI: https://doi.org/10.54028/NJ202322315

Tominaga, Y, Mochida, A, Yoshie, R, Kataoka, H, Nozu, T, Yoshikawa, M and Shirasawa, T. 2008. AIJ guidelines for practical applications of CFD to pedestrian wind environment around buildings. Journal of Wind Engineering and Industrial Aerodynamics, 96: 1749–1761. DOI: https://doi.org/10.1016/j.jweia.2008.02.058

Tong, S, Wen, J, Wong, NH ang Tan, E. 2021. Impact of façade design on indoor air temperatures and cooling loads

in residential buildings in the tropical climate. Energy and Buildings, 243: 110972. DOI: https://doi.org/10.1016/j.enbuild.2021.110972

U.S. Centers for Disease Control and Prevention (U.S. CDC), 2024 About Ventilation and Respiratory Viruses, 3 October 2024. Available at https://www.cdc.gov/niosh/ventilation/prevention/Aim-for-5.html [Last accessed 23 December 2024].

United Nations, Department of Economic and Social Affairs, Population Division 2019 World urbanization prospects: The 2018 Revision. New York: United Nations.

van Hooff, T, Blocken, B and Yoshihide, T. 2016. On the accuracy of CFD simulations of cross-ventilation flows for a generic isolated building: comparison of RANS, LES and experiments. Building and Environment, 114: 148-165, DOI: 10.1016/j.buildenv.2016.12.019.

World Health Organization (WHO), 2021 Coronavirus disease (COVID-19): Ventilation and air conditioning, 23 December 2021. Available at https://www.who.int/news-room/questions-and-answers/item/coronavirus-disease-covid-19-ventilation-and-air-conditioning [Last accessed 14 August 2024].

Zhang, Z, Wei, Y, Wang, T, Li, Y, Zhong, Y and Zhang, G. 2021. Potential of cross-ventilation channels in an ideal typical apartment building predicted by CFD and multi-zone airflow mode. Journal of Building Engineering, 44: 103408. DOI: https://doi.org/10.1016/j.jobe.2021.103408

Zhao, Y, Liu, Z, Li, X, Zhao, M and Liu, V. 2020. A modified turbulence model for simulating airflow aircraft cabin environment with mixed convection. Building Simulation, 13(3): 665-675. DOI: 10.1007/s12273-020-0609-2.

Zhong, W, Zhang, T and Tamura, T. 2019. CFD simulation of convective heat transfer on vernacular sustainable architecture: validation and application of Methodology. Sustainability, 11: 4231. DOI: https://doi.org/10.3390/su11154231

Zhou, C, Wang, Z, Chen, Q, Jiang, Y and Pei, J. 2014. Design optimization and field demonstration of natural ventilation for high-rise residential buildings. Energy and Buildings, 82: 457-465. DOI: https://doi.org/10.1016/j.enbuild.2014.06.036